Melanoma Activation of 3-*O*-(3,4,5-Trimethoxybenzoyl)-(-)-Epicatechin to a Potent Irreversible Inhibitor of Dihydrofolate Reductase

Luís Sánchez-del-Campo[†], Alberto Tárraga[‡], María F. Montenegro[†], Juan Cabezas-Herrera[§], and José Neptuno Rodríguez-López*[,†]

Department of Biochemistry and Molecular Biology A, School of Biology, University of Murcia, Murcia, Spain, Department of Organic Chemistry, Faculty of Chemistry, University of Murcia, Murcia, Spain, Research Unit of Clinical Analysis Service, University Hospital Virgen de la Arrixaca, Murcia, Spain

*Corresponding author. Mailing address: Department of Biochemistry and Molecular Biology A, School of Biology, University of Murcia, 30100 Murcia, Spain. E-mail: neptuno@um.es. Tel: +34-968 398284. Fax: +34-968 364147.

[†]Department of Biochemistry and Molecular Biology A, School of Biology, University of Murcia, Murcia, Spain.

[‡]Department of Organic Chemistry, Faculty of Chemistry, University of Murcia, Murcia, Spain.

[§]Research Unit of Clinical Analysis Service, University Hospital Virgen de la Arrixaca, Murcia, Spain.

Running title: *New antifolate prodrug against melanoma*

Abstract: Human melanoma is a significant clinical problem because it is resistant to treatment by most chemotherapeutic agents, including antifolates. It is therefore a desirable goal to develop a second generation of low-toxicity antifolate drugs to overcome acquired resistance to the prevention and treatment of this skin pathology. In our efforts to improve the stability and bioavailability of green tea polyphenols for cancer therapy, we synthesized a trimethoxy derivative of epicatechin-3-gallate, which showed high antiproliferative and pro-apoptotic activity against melanoma. This derivative, 3-*O*-(3,4,5-trimethoxybenzoyl)-(-)-epicatechin (TMECG), is a prodrug that is selectively activated by the specific melanocyte enzyme tyrosinase. Upon activation, TMECG generates a stable quinone methide product that strongly inhibits dihydrofolate reductase in an irreversible manner. The treatment of melanoma cells with TMECG also affected cellular folate transport and the gene expression of DHFR, which supported the antifolate nature of this compound. In addition, its pharmacological efficacy has been confirmed in a mouse melanoma model, in which tumor growth and metastasis were inhibited, significantly enhancing the mean survival of the treated groups. TMECG, therefore, shows a potential for clinical use in melanoma therapy.

Keywords: melanoma; dihydrofolate reductase; antifolates; prodrug activation

Introduction

Cancer remains a frequent cause of death even though several standard and experimental treatments have been developed. These include surgery, chemotherapy, radiotherapy, biotherapy and immunotherapy. In particular, the incidence rates of melanoma have risen faster than that of any other malignancy in the Caucasian populations over the past 30 years.[1] According to a World Health Organization estimate, there are 132,000 new cases of melanoma per year worldwide. Light skin, large numbers of nevi and excessive sun exposure, especially in childhood, are the major factors that contribute to melanoma risk.[2] Primary melanomas, once detected, should be surgically removed, while chemotherapy should focus on metastasis control. At present, limited therapeutic options exist for patients with metastatic melanomas, and all standard combinations currently used in metastasis therapy have low efficacy and poor response rates.[3] An example of the difficulty involved in melanoma chemotherapy is the limited effect of antifolates. Although methotrexate (MTX), the most frequently used antifolate, is an efficient drug for several types of cancer it is not active against melanoma.[4] The nature of the resistance of melanoma cells to MTX is as yet unclear but seems to be related to several general mechanisms, including the reduced cellular uptake of the drug, insufficient cellular retention, metabolic MTX inactivation, and/or enhanced intracellular levels of DHFR.[4-6] It is therefore of great interest to develop a second generation of antifolate drugs that overcome these problems and present low toxicity for the prophylaxis and treatment of melanoma.

Recently, we have shown that the ester-bonded gallate catechins isolated from green tea, epigallocatechin-3-gallate (EGCG) and epicatechin-3-gallate (ECG), are potent inhibitors of dihydrofolate reductase (DHFR) activity *in vitro* at concentrations found in the serum and tissues of green tea drinkers.[7] Since this first report describing the antifolate activity of tea polyphenols, several studies from other laboratories have confirmed such activity[8] and

reported that EGCG inhibits DHFR obtained from different biological sources.[9-11] Recently, a screening of DHFR-binding drugs by MALDI-TOFMS demonstrated that EGCG is an active inhibitor of DHFR, with a relative affinity between those of pyrimethamine and MTX.[11] However, despite the excellent anticancer properties of tea catechins, they have at least one significant limitation: their poor bioavailability, which is related to their low stability in neutral or slightly alkaline solutions and their inability to cross cellular membranes easily.[12] In an attempt to solve such bioavailability problems, we synthesized a 3,4,5-trimethoxybenzoyl analogue of ECG (TMECG), which showed high antiproliferative activity against malignant melanoma.[13] Recently, we observed that this compound effectively suppressed the proliferation of melanoma cells in cultures by inducing apoptosis.[14] TMECG treatment of melanoma cells resulted in the downregulation of antiapoptotic Bcl-2, the upregulation of proapoptotic Bax and the activation of caspase-3.[14] Therefore, the aim of this study was to investigate the origin of the specificity of TMECG in malignant melanoma and the mechanism/s by which it exerts its antiproliferative action. In addition, we provide evidence that explains how TMECG evades the natural mechanisms of resistance to classical antifolates in melanoma.

Materials and Methods

Reagents. Epicatechin (EC; > 98%), ECG (> 98%), NADPH, MTX, 1-ethyl-3-(3-dimethylaminopropyl)-carbodiimide (EDC), folic acid and fluorescein isothiocyanate (FITC) were obtained from Sigma (Madrid, Spain) and DHF (90%) was from Aldrich (Madrid, Spain). TMECG was synthesized from catechin with the subsequent inversion of the stereochemistry at C-3 and by reaction with 3,4,5-trimethoxybenzoylchloride.[11] Mushroom TYR (Sigma) was used to synthesize the quinone methide (QM) related product. Recombinant human DHFR (rHDHFR) was purchased from Sigma and its concentration was determined by MTX titration of enzyme fluorescence.[15] Anti-TYR, anti-reduced folate

carrier (anti-RFC) and anti-DHFR were from Santa Cruz Biotechnology (Santa Cruz, CA, USA). 3-(4,5-dimethylthiazol-2-yl)-2,5-diphenyl-tetrazolium bromide (MTT) was from Sigma and 3-(4,5-dimethylthiazol-2-yl)-5-(3-carboxy-methoxyphenyl)-2-(4-sulfophenyl)-2H-tetrazolium (MTS) was from Promega Biotech Iberica (Barcelona, Spain).

Cells, Proliferation and Apoptosis Assays. Human and mouse cancer cell lines were obtained from the American Type Culture Collection (ATCC) and were maintained in appropriate culture media under standard tissue culture conditions. HeM were supplied by Gentaur (Brussels, Belgium) and were cultured in HAM-F10 medium supplemented with 10% fetal calf serum, antibiotics and the human melanocyte growth supplement (Gentaur). Hypoxanthine-thymine medium (HT-medium) was purchased from Sigma. Cell viability was evaluated using the MTT and MTS cell proliferation assays for adherent and suspended cells, respectively. Apoptosis induction was assessed by analysis of cytoplasmic histone-associated DNA fragmentation using a kit from Roche Diagnostics (Barcelona, Spain). Apoptosis is represented as the specific enrichment of mono- and oligonucleosomes released into the cytoplasm and was calculated by dividing the absorbance of treated samples by the absorbance of untreated controls.

Cellular Uptake of Catechins. Cellular uptake of catechin was determined by the difference between the initial concentration of catechin and the calculated concentration at specific times in the cellular medium, and expressed as a percentage of catechin at time zero. Catechin concentrations were determined by HPLC analysis.[13] Catechins were identified by their characteristic elution times and their concentrations were calculated with respect to calibration curves for known concentrations of catechins.

Folate Conjugation with TYR and Fluorescent Labeling. Folic acid (10 mM) was completely dissolved in a pH 9.0 buffer solution (100 mM, carbonate buffer) and then an equimolar quantity of EDC (10 mM) was added. The mixture was stirred for 40 min at room

temperature. The activated folate (1 mL) was added to 10 μM mushroom TYR solutions (1mL, pH 9.0) and incubated for 18 h at room temperature. The folate-conjugated proteins were separated from unreacted folate using a Sephadex G-25 desalting column equilibrated in PBS (pH 7.4). The degree of folate conjugation was determined spectro-photometrically by measuring the difference in absorbance between the conjugated and free proteins at 363 nm (folate, $\varepsilon = 6197\ M^{-1}cm^{-1}$ in PBS, pH 7.4). Free TYR and folate-conjugated TYR (FOL-TYR) were dissolved in a pH 9.0 buffer solution (100 mM, carbonate buffer) and 50 μL of a 10 mg/mL FITC solution (in DMSO) was added and mixed for 2 h at room temperature. TYR-FITC and FOL-TYR-FITC were separated from unreacted FITC using a Sephadex G-25 desalting column equilibrated in PBS (pH 7.4). FITC incorporation was determined by fluorescent emission spectroscopy. The activity of folate-conjugated TYR was determined by measuring aminochrome formation using L-DOPA as an enzyme substrate. A solution containing either folate-conjugated TYR or free TYR (50 μL, either 30 μg/mL) was mixed with 0.95 ml of 0.2 mM L-DOPA in a pH 7.4 buffer solution (50 mM, phosphate buffer) and the absorbance was monitored at 475 nm.

Cellular Uptake of Folate-Conjugated TYR. Caco-2 cells were incubated with either 25 μg/mL FITC-TYR or the same TYR concentration of FOL-TYR-FITC for 4 h. The cells were washed three times with PBS and analyzed by confocal microscopy (Leica TCS 4D, Wetzlar, Germany) and flow cytometry (Beckman-Coulter EPICS XL, Fullerton, CA, USA). To investigate the activation of TMECG by TYR, Caco-2 cells were preloaded with 10 μM TMECG for 3 days. After washing the cells three times with medium, the cells were exposed to FOL-TYR (25 μg/mL) for 8 h under culture conditions. Then the enzyme was removed from the medium by extensive washing and cells were incubated with 10 μM TMECG for another 5 days.

TYR siRNA Gene Silencing. TYR expression was knocked down using specific human siRNAs (Santa Cruz Biotechnologies) and LipofectAMINE 2000 (Invitrogen, Barcelona, Spain) using standard protocols specified by the suppliers. Briefly, SkMel-28 cells were seeded in 96-well plates in Opti-MEM medium one day before transfection. In each well, 83 nM siRNA duplexes diluted in serum-free medium were incubated with 2 μL of LipofectAMINE 2000 for 20 min at room temperature. Then, 100 μL mixture per well were added to the cells and incubated at 37°C. Treatments started 24 h after siRNA transfection. For each condition tested, a negative siRNA control (siRNA CN) was used (Santa Cruz Biotechnology). Validation of RNA gene silencing was measured by quantitative PCR and western blot analysis at 24 and 72 h after siRNA transfection.

TYR Assays. Human TYR was purified to homogeneity[16] from SkMel-28 (1×10^8 cells). TMECG oxidation catalyzed by human TYR was followed at 412 nm using a Perkin-Elmer Lambda-35 spectrophotometer (Waltham, MA, USA).

DHFR Inhibition and Binding Assays. Kinetic experiments were carried out in a buffer containing 2-(*N*-morpholino)ethanesulfonic acid (Mes, 25 mM), sodium acetate (25 mM), tris-(hydroxymethyl)aminomethane (Tris 50 mM), and NaCl (0.1 M) at pH 7.4 and 25ºC. Inhibition constants for rHDHFR were calculated as previously described[17] using NADPH (100 μM), DHF (10 μM), and rHDHFR (1.5 nM). The dissociation constant for the binding of inhibitors to free rHDHFR was determined by fluorescence titration in a Perkin-Elmer LS50B spectrofluorimeter. Stopped-flow fluorescence experiments were carried out using an Applied Photophysics Pi-Star 180 spectrometer (Surrey, UK). Stopped-flow fluorescence experiments were carried out using an enzyme concentration of 0.25 μM. The reaction of rHDHFR with inhibitors was observed under pseudo-first order conditions by fluorescence at 340 nm (excitation at 290 nm). To study the recovery of the rHDHFR activity after preincubation with TMECG or QM, rHDHFR (75 nM) was preincubated for 30 min at 25ºC

in the buffer medium containing 10 μM inhibitors. Aliquots (20 μL) of the incubation mixture were then diluted 50-fold into a reaction mixture containing the buffer, NADPH (100 μM), and DHF (10 μM) to give a final enzyme concentration of 1.5 nM.

In Silico Molecular Modeling. Molecular modeling was carried out using the CAChe software package v.7.5 (Fujitsu, Krakow, Poland). In searching for the available ligand-bound human DHFR structures in the PDB,[18] we identified a 1.8 Å structure (accession code 1S3V)[19] was the best available structural match for TMECG or QM. Using the position of (R)-6-{[methyl-(3,4,5-trimethoxyphenyl)-amino]methyl}-5,6,7,8-tetrahydroquinazoline-2,4-diamine as a guide, compounds were docked into this protein structure and the inhibitor-protein composite was then energy minimized.

Western Blot Analysis. Cells were lysed by sonication in PBS pH 7.4 containing 1% NP-40, 1% Triton X-100, 0.5% sodium deoxycholate, 0.1% SDS, 1 mM PMSF and protease inhibitor cocktails. After centrifugation (100,000 *g*, 10 min), extracted proteins were separated by SDS-PAGE, transferred to nitrocellulose membranes, and analyzed by immunoblotting (ECL Plus, GE Healthcare).

Quantitative Real-Time PCR Analysis. RT-PCR analysis was carried out as described elsewhere,[14] using the following primers for the amplification of human (h) and mouse (m) genes: *h-DHFR* (forward: 5'-ATG CCT TAA AAC TTA CTG AAC AAC CA-3'; reverse: 5'-TGG GTG ATT CAT GGC TTC CT-3'); *h-TYR* (forward: 5'-TTG GCA GAT TGT CTG TAG CC-3'; reverse: 5'-AGG CAT TGT GCA TGC TGC TT-3'); *m-TYR* (forward: 5'-GGG CCC AAA TTG TAC AGA GA-3'; reverse: 5'-ATG GGT GTT GAC CCA TTG TT-3'); *h-RFC* (forward: 5'-ACC GAC TAC CTG CGC TAC AC-3'; reverse: 5'-CCG CAC GAG AGA GAA GAT GT-3') and *m*- and *h-β-actin* (forward: 5'-AGA AAA TCT GGC ACC ACA CC-3'; reverse: 5'-GGG GTG TTG AAG GTC TCA AA-3').

Mouse Tumor Model. Female C57/B16 mice 6 - 8 weeks old were obtained from the Animal Research Service (University of Murcia, Spain). They were bred and kept according to the Spanish legislation on 'Protection of Animals used for Experimental and other Scientific Purposes,' and in accordance with the Directives of the European Community on this issue. The B16 melanoma cell line (ATCC) was cultured in RPMI 1640 medium under standard tissue culture conditions. Mice were shaved on the back using a long-hair cutter and 7.5×10^5 B16 melanoma cells resuspended in 25 μL sterile PBS were injected intradermally in the back of the animals. Animals with tumors more than 8 mm in diameter on day 8 or no visible tumor growth by day 12 were excluded. Groups (20 mice per group) were differently treated starting at day 8 after tumor cell injection. For TMECG and MTX treatments these compounds were uniformly mixed in a cosmetic base cream. Topical treatment with these drugs was provided every day at a dose of ≈ 1 mg/cm^2 skin area. Control mice (non- treated) were topically treated with the some amount of cream alone. Tumor growth and body weight were monitored every other day. In experiments to assess survival, mice were killed when they became moribund. To explore the toxicity of TMECG and MTX, these drugs (both at 10 mg/kg/day) were individually administrated intradermally to the back of non-tumor inoculated mice (n = 10), and the body weight was monitored every other day. A postmortem with histological examination of the lungs was performed in all animals. Tissues were fixed in 10% formaldehyde, dehydrated and embedded in paraffin wax. Sections (4 μm) were stained with eosin and hematoxylin.

Statistical Analysis. In all experiments, the mean ± standard deviations (SD) for 5 determinations in triplicate were calculated. Statistically significant differences were evaluated using the Student's *t*-test. Differences were considered statistically significant at $p < 0.05$.

Results

TMECG Is More Effective Against Melanoma Cells. In comparing the antiproliferative activity of TMECG (expressed as its half maximal inhibitory concentration, IC_{50}) on several human and mouse cancer cell lines, we noticed that this compound was much more active on melanoma cells (SkMel-28, SkMel-1, G361, and B16/F10 with IC_{50} at seven days at 2.9, 1.3, 2.1 and 0.9 μM, respectively) than on normal melanocytes (HeM) and other epithelial cancer cell lines from breast (MCF7), lung (H1264) and colon cancers (Caco-2) (Figure 1a). A linear relationship was observed between the TMECG IC_{50}-value and the doubling time for non-melanoma cells; however, TMECG was more active against SkMel-28, which exhibited the lowest doubling time (Figure 1a). To understand the varying degrees of TMECG activity on different cells, we first searched for differences in its cellular uptake. Although the transport of TMECG was faster than the uptake of its related natural catechin (ECG), in all tested cells, no significant differences were observed in TMECG transport through the membrane of epithelial cells (Supporting Information Figure S1). Next, we compared the activity of TMECG with the activity of two natural tea catechins using SkMel-28 and Caco-2 cells. EC showed no detectable activity against either cellular system, while responses to ECG and TMECG were different. Caco-2 showed similar sensitivity to both compounds, while the growth of SkMel-28 was highly inhibited by TMECG but not ECG (Supporting Information Figure S2a). SkMel-28 cells exposed to 20 μM TMECG for five days showed evidence of apoptosis; however, the only appreciable difference after treatment with ECG was the presence of a greater amount of black pigment inside the cells (Supporting Information Figure S2b); this was probably associated with a higher melanin cell content.

TMECG Is Activated by TYR. Next, we designed experiments to throw light on the elevated activity of TMECG on melanoma cell lines. As one of the most striking differences

between melanoma and other epithelial cells is the presence of TYR in melanoma, we wondered whether TMECG cytotoxicity against melanoma might be mediated by cellular TYR activation. This hypothesis would explain the low activity of TMECG in breast, lung and colon cancer cells; however, normal melanocytes expressing this enzyme were also more resistant to TMECG treatments than malignant melanocytes (Figure 1a). We first analyzed the levels of TYR expression in melanoma cells, which were compared with its levels in HeM. As shown in Figure 1b, TYR mRNA and protein were highly overexpressed in all types of melanoma cell lines. A change in cell mobility, which is one of the preconditions of tumor metastasis, and the loss of pigmentation are common characteristics in metastatic melanoma cells. Here, we show that TYR expression levels and TMECG cytotoxicity are high in suspension (SkMel-1) and amelanotic (SkMel-28) cells, which could represent models for melanoma metastatic cells. The data also indicated that normal melanocytes containing low levels of TYR expression were highly resistant to TMECG treatment, which is a highly desirable feature for potential antitumoral agents.

To prove that TMECG activity against melanoma was mediated by cellular TYR activation, we used two different experimental approaches. First, we silenced TYR expression using siRNA and observed that the antiproliferative action of TMECG on SkMel-28 cells was mitigated after TYR silencing (Figure 2a). Second, we designed strategies to deliver TYR into Caco-2 colorectal cancer cells and investigated the ability of this enzyme to enhance the antiproliferative effect of TMECG on this cell line. A method that exploits folate receptor α (FRα) endocytosis has been successfully employed to deliver active proteins into living cells.[20] As Caco-2 cells constitutively express the FRα,[21] folate was conjugated to mushroom TYR using EDC chemistry (Supporting Information Results and Figure S3), and the complex FOL-TYR was used to deliver the enzyme into Caco-2 cells. The efficient uptake of FOL-TYR into Caco-2 cells was confirmed by confocal microscopy

and flow cytometry, which compared the internal fluorescence of Caco-2 cells incubated with either fluorescein-labeled FOL-TYR or fluorescein-labeled TYR. As shown in Figure 2b, the uptake of folate-conjugated TYR was 4.2-fold greater than that of free TYR, suggesting that enhanced endocytosis of FOL-TYR is partially responsible for its greater transport efficacy. The presence of TYR in the cytoplasm of Caco-2 cells strongly enhanced the activity of TMECG, inducing cell growth inhibition and apoptosis (Figure 2c). Together the results indicate that TMECG activation by TYR might explain its greater effects on melanoma cells.

Mechanism of TMECG Activation by TYR. Active TYR is localized in the membrane of melanosomes, which are oval pigment granules produced by melanocytes. Due to strong experimental evidence that the intracellular pH of melanosomes is acidic,[22] we decided to study the oxidation of TMECG by TYR at pH 5.5. As can be seen in Figure 3a, TMECG was efficiently oxidized by human TYR. The Michaelis-Menten constant (K_m) of TYR for TMECG was 0.12 ± 0.02 mM (Figure 3b), which was similar to the value reported for L-dopa (0.36 mM), using recombinant human TYR.[23] It is well known that the *o*-quinones are the primary products of the oxidation of *o*-diphenols catalyzed by TYR.[24] The oxidation of TMECG by TYR at pH 5.5 produced an *o*-quinone (*o*-Q), which was detected within a few seconds after the reaction began. This intermediate (λ_{max} = 400 nm) quickly evolved to a yellowish product with a λ_{max} at 412 nm. The initial formation of *o*-Q was confirmed by including reducing agents such as ascorbic acid or NADPH in the reaction medium. The oxidation of TMECG by TYR in the presence of ascorbic acid or NADPH involved a lag period proportional to the concentration of reductant (data not shown), indicating that the *o*-Q was effectively reduced by these two chemical agents. The final product of the TYR reaction, in contrast, was highly stable and was not reduced by ascorbic acid or NADPH. At basic pH values, its color changed from yellow to orange with an intense visible band at 470

nm. The presence of an ionizable group with a pK_a of 6.9 ± 0.1 (Figure 3c) helped us to identify its structure. By analogy with the copper(II)-mediated oxidation of quercetin,[25] the proposed structure for this compound is depicted in Chart 1 and was identified as a quinone methide (QM), which is formed by proton-catalyzed hydrolysis of ring-C. The pH transition might represent the equilibrium between the protonated form (QMH) and the deprotonated form ($QM^{\ominus}$), a species that is stabilized by resonance. The anionic nature of this product may also be deduced from its limited diffusion across cell membranes (Supporting Information Figure S1). Chart 1 also depicts the possible abundance of QM species in different melanocyte compartments.

QM Is an Irreversible Inhibitor of Human DHFR. Green tea catechins containing an ester-bound gallate moiety are potent inhibitors of mammalian DHFRs.[7] The synthetic catechin, TMECG, also inhibited recombinant human DHFR (rHDHFR) with an effective inhibition constant (K_I^*) of 0.11 μM (Table 1). Mushroom TYR was used to synthesize the QM and its affinity for rHDHFR at pH 7.4 was assayed by measuring fluorescence quenching (Figure 4a). The binding of QM quenched rHDHFR fluorescence with a dissociation constant (K_I) of 8.2 ± 0.11 nM. Compared with other inhibitors of rHDHFR, QM showed intermediate affinity between MTX and catechins; QM bound more than two orders of magnitude more strongly than catechins but forty times less strongly than MTX (Table 1). When the activity was continuously assayed after addition of the enzyme to mixtures containing QM and enzyme substrates, the resulting progress curves were representative of irreversible inhibition (Figure 4b).[26] The binding of TMECG and QM to free enzymes was investigated at pH 7.4 using stopped-flow fluorescence kinetics. Under pseudo first-order conditions, the apparent rate of reaction increased linearly with inhibitor concentration and showed no evidence of saturation at higher concentrations (Figure 4c). Assuming a simple association step, the observed rate (k_{obs}) may be approximated by the

relationship, $k_{obs} = k_{on}[I] + k_{off}$, where k_{on} and k_{off} are the rate constants for the association and dissociation, respectively. Thus, a plot of k_{obs} against [I] gave a straight line of slope k_{on} and intercept k_{off} (Figure 4c). Following this scheme, second-order rate constants were obtained for the reaction of rHDHFR with TMECG or QM (Table 1). In each of these experiments the intercept value of k_{off} was too small to be measured, although it could be calculated from the K_I expression ($K_I = k_{off} / k_{on}$) (Table 1). As shown in this table, the association constants of rHDHFR for TMECG and QM are of the same order, while the first-order rate constant for the dissociation of QM to the free enzyme is around 3 orders of magnitude lower than that of TMECG, which makes the binding of QM to rHDHFR essentially irreversible. Further evidence for this irreversibility was obtained by comparing the effect of adding aliquots of pre-incubation mixtures of rHDHFR with QM or TMECG to assay mixtures containing substrates (Figure 4d). The high irreversibility in the binding of QM to rHDHFR also conditioned its action mechanism, which differed from the other compounds assayed. MTX and tea catechins act as slow-binding inhibitors of rHDHFR,[17,27] so the overall inhibition constant (K_I^*) is decreased by further EI-complex reactions (Table 1).

To explain the irreversibility on the binding of QM to rHDHFR, we performed *in-silico* molecular modeling experiments. TMECG bound to human DHFR in a similar way to that described for EGCG binding,[7] with specific hydrogen bonding interactions, most notably involving Glu-30 (Figure 4e). However, the open structure of QM increases its molecular flexibility, and it adopts a different conformation in the active site of human DHFR (Figure 4e). QM maintained the hydrogen bond with the Glu-30 side chain (O···O distance 1.99 Å), but three new interactions were detected. The other phenolic group of ring A forms a hydrogen bond with Ile-7, whereas the other two hydrogen bonds formed between two

oxygens of the methoxy groups of ring D and Ser-59 and Ile-60. This strong interaction between QM and different residues of the protein could explain the irreversibility of the inhibitor-protein complex, although mutation of these residues by site directed mutagenesis would be desirable to validate this hypothesis.

TMECG Modulates SkMel-28 Folate Transport. Having demonstrated the strong *in vitro* inhibition of rHDHFR by QM, further experiments were designed to test its antifolate activity in culture systems. It is widely accepted that antifolates block the *de novo* biosynthesis of thymine, purines and pyrimidines by inhibiting the synthesis of THF, an essential cofactor in these biosynthetic pathways, and that the administration of exogenous reduced folates, such as leucovorin (5-formyl-THF), or growing the cells in an HT-medium, effectively prevent antifolate cytotoxicity in mammalian cells. Figure 5a shows a different effect of leucovorin and HT-medium in the reversion of the TMECG effects on SkMel-28. TMECG was more active on cells growing in a normal culture medium than in an HT medium (Figure 5a). However, leucovorin did not "rescue" SkMel-28 cells from TMECG-induced death (Figure 5a). Recently, it has been reported that natural tea catechins inhibit folate transport in Caco-2 cells, which might be partly responsible for their antifolate activity.[8] Therefore, to understand the different response of SkMel-28 to leucovorin- and HT-treatments, and to prove or discard the *in vivo* antifolate activity of TMECG, the status of the RFC, the major protein involved in the transport of reduced folates, was analyzed in this cell line. RFC mRNA expression was significantly higher in SkMel-28 than in HeM cells (8.9 times) (Figure 5b). Treating SkMel-28 with TMECG strongly downregulated RFC gene expression (Figure 5b). The time-dependent effect of TMECG on SkMel-28 was studied using RT PCR (Figure 5b), and the data indicated that cells responded quickly to TMECG treatment with a more than 80% reduction in RFC expression 24 h after treatment. Protein levels of this transporter correlated with gene expression (Figure 5b). This finding

could explain why leucovorin did not affect TMECG treatments. As demonstrated here, TMECG highly down-regulated the RFC and, therefore, SkMel-28 cells became practically impermeable to leucovorin during TMECG treatment and can not, therefore, restore the reduced folate levels in the cells.

TMECG Efficiently Down-Regulates Melanoma DHFR Expression. As described for several melanoma tumors and other cancer cell lines,[4] DHFR is overexpressed in SkMel-28 cells (Figure 5c). The level of DHFR polyA$^+$ mRNA in these melanoma cells was estimated to be 400 to 500 times higher than in HeM cells, resulting in increased DHFR protein content (Figure 5c). An increase in DHFR expression/activity after antifolate treatment has been recognized as a mechanism of resistance of cancer cells to antineoplastic drugs. As expected, treatment of SkMel-28 with MTX resulted in a significant increase of DHFR mRNA and protein (Figure 5c). However, treatment of SkMel-28 with TMECG rapidly reduced DHFR mRNA and protein to normal levels (Figure 5c). The efficient down-regulation of DHFR by TMECG is evidence of its proposed antifolate activity. The lack of reduced folate coenzyme recycling by DHFR could be one of the reasons for its *in vivo* activity.

TMEGC Inhibits Growth and Metastasis of Induced Melanoma Tumors in Mice. A paradoxical response of malignant melanoma to MTX *in vivo* and *in vitro* has been described.[28] The authors observed that MTX showed consistent cytotoxicity for melanoma cells *in vitro* but was ineffective at equivalent concentrations *in vivo*. Inactivation of MTX to 7-hydroxy-MTX (7-OH-MTX) in the liver was proposed as a novel mechanism of resistance to explain this paradox.[6,28] To check whether TMECG was pharmacologically active in *in vivo* situations and to study the possible inactivation of TMECG in the body, we performed experiments to test the effectiveness of this compound in induced melanoma tumors in mice. The group receiving TMECG therapy showed significantly longer survival times than the

control group (Figure 6a). To confirm whether the lower survival of MTX-treated animals was related with the well known toxicity of this drug, MTX and TMECG were administrated to tumor-free mice and their respective toxicities assessed by determining body weights (Figure S4). Moreover, we observed that tumor growth was significantly reduced by the treatment with TMECG but not with MTX (Figure 6b). The observation that TMECG-treated animals survived with larger tumors indicated that treatment could also reduce the metastasis of primary tumors. To confirm this, a third group was inoculated with B16 melanoma cells and treated with TMECG for 21 days (median survival time of the control group). After this time the animals were sacrificed and a post-mortem examination of the lungs was performed to search for metastatic lesions. Secondary metastasis in the lungs was more frequent in control mice (Figure 6c), while treatment with TMECG drastically reduced lung metastasis. The lungs of the control animals showed prominent tumor nodules around the terminal bronchioles. These tumor nodules were composed of polygonal tumor cells with a prominent nucleolus. Intracellular melanin deposition and clear areas of necrosis were also detected. The lungs of the TMECG-treated tumor-bearing animals showed no significant tumor mass. The alveoli and pleura were tumor free, and the alveolar passage was lined with healthy ciliated columnar epithelial cells.

Discussion

Some catechins, such as ECG or EGCG, inhibit cancer cell proliferation.[29] To avoid therapeutic problems associated with their poor stability and low cellular uptake, the variant compound TMECG was synthesized.[13] The observation that its effectiveness was directly correlated with doubling time in HeM, H1264, Caco-2 and MCF7 cells indicated that TMECG may affect cell growth by depleting cellular stores of molecules essential for cell survival, particularly in cells with faster metabolism. However, another aspect must be taken into consideration in melanoma cells: since expression of TYR, the enzyme responsible for

melanin biosynthesis,[30] has been found highly increased in melanoma cells, the activation of TMECG by this enzyme may explain its intracellular activation. Kinetic and spectroscopic data indicated that TYR oxidized TMECG to its corresponding *o*-quinone, which quickly evolved through a series of chemical reactions to a quinone methide (QM), which showed high stability over a wide pH range. Thus, the data suggest that this highly stable product may be responsible for the observed high activity of TMECG on melanoma cells. This hypothesis was confirmed by experiments showing that delivery of TYR in the nonmelanotic Caco-2 cell line strongly increased the pro-apoptotic activity of TMECG. The action of TYR on TMECG would not only explain why this synthetic catechin is activated, but also why melanoma cells are essentially resistant to ECG. Although ECG is also effectively oxidized by TYR, the enzymatically generated product may undergo multiple coupled reactions as a result of the presence of multiple phenolic groups in the ester-bound gallate moiety. These reactions may facilitate its incorporation in melanin, as demonstrated by the strong pigmentation of the cells treated with ECG, thus preventing its antiproliferative action.

A mechanism for the activation, cellular distribution and action of TMECG and its products may now be proposed. Although TMECG efficiently binds to DHFR, we hypothesized that this hydrophobic compound would cross the cell membrane without needing to bind to folate transporters. Therefore, the most plausible transport mechanism for this lipophilic drug is passive diffusion across the plasma membrane in a manner driven solely by the concentration gradient. Its independence from folate transporters means that TMECG may avoid transport-mediated resistance mechanisms.[31] In fact, TMECG downregulated RFC but, far from being a disadvantage, this could represent an important advantage for its antiproliferative action. Downregulation of RFC would reduce intracellular folate pools, reducing competition reactions with the active form of TMECG and the

molecular target, DHFR. Subsequent transport to the melanosome by a concentration gradient would facilitate its TYR-catalyzed oxidation and transformation to the corresponding QM. Because of the low pH of this organelle, the predominant form is QMH, which, due to its high stability and the absence of formal charge, would exit the melanosome and enter the cytosol. Under the slightly basic pH of the cytosol, $QM^{\ominus}$ would be the predominant form, and it would be trapped in this compartment due to its formal negative charge. This retention mechanism would represent another advantage with respect to antifolates that require polyglutamylation for cellular retention. This would be even more essential in cancer cell environments, in which folate requirements lead to an increase in the cellular THF-cofactor pools. As the THF-cofactor pool is increased, there is a feedback inhibition of folate polyglutamylation, which results in the accumulation of easily exported compounds.[32] Once in the cytosol, TMECG may inhibit DHFR activity and, in addition, lead to the downregulation of DHFR. The finding that TYR is highly overexpressed in melanoma cells with respect to normal melanocytes might also influence the degree, the specificity and the duration of the antifolate inhibitory effect of TMECG. Finally, the data on the effectiveness of TMECG in mouse melanoma models indicates that TMECG is bioavailable for cancer cells and avoids not only cellular mechanisms of resistance to antifolates but also mechanisms related with body drug inactivation.

Conclusion

In conclusion, we have demonstrated that a synthetic derivative of ECG, TMECG, might be considered a treatment for melanoma. Disruption of the cell folate cycle by TMECG and its active products may explain many of the molecular and cellular effects described for this synthetic polyphenol on melanoma cells because antifolates exert their action by disturbing the nucleic acid metabolism of cancer cells, including its synthesis, methylation and stability.[14,33] We define it as a *new generation antifolate* because it

maintains the ability to inhibit DHFR and disrupt folate metabolism but shows significant and important differences from other classical and non-classical antifolates. This compound was seen to be active not only in melanoma cells in culture but was also effective in an animal model, where it inhibited growth and metastasis of preformed tumors. Prodrugs are compounds that must be transformed before exhibiting their pharmacological action. They are often divided into two groups: those designed to increase bioavailability to improve the pharmacokinetics of antitumor agents, and those designed to deliver antitumor agents locally.[34] TMECG could therefore, be considered an anticancer prodrug since it showed both of these characteristics. Therapies with TMECG would increase bioavailability and would achieve high melanoma drug concentrations. The soft antifolate character[35] of the prodrug (TMECG), its specific activation on melanoma cells and the fact that antifolates are more active on fast-dividing cancer cells make this compound ideal for the prevention and treatment of this skin pathology.

Acknowledgments. This work was supported in part by grants from PBL International and Ministerio de Educación y Ciencia (Project SAF2006-07040-C02-01) to J.N.R-L, from Ministerio de Educación y Ciencia (Project SAF2006-07040-C02-02) to J.C-H and from Fundación Séneca (Comunidad Autónoma de Murcia) (Project 02970/PI/05) to A.T. L.S-d-C has a contract from the Conserjería de Educación, Ciencia e Investigación (Comunidad Autónoma de Murcia) (Project BIO-BMC 07/03-009).

Supporting Information Available: Additional results of the folate and FITC conjugation to mushroom TYR and four additional Figures. The material is available free of charge via the Internet at http://pubs.acs.org.

References

(1) Giblin, A.V.; Thomas, J.M. Incidence, mortality and survival in cutaneous melanoma. *J. Plast. Reconstr. Aesthet. Surg.* **2007**, *60*, 32–40.

(2) Houghon, A.N.; Polsky, D. Focus on melanoma. *Cancer Cell* **2002**, *2*, 275-278.

(3) Koon, H.; Atkins, M. Autoimmunity and immunotherapy for cancer. *N. Engl. J. Med.* **2006**, *354*, 758-760.

(4) Kufe, D.W.; Wick, M.M.; Abelson, H.T. Natural resistance to methotrexate in human melanomas. *J. Invest. Dermatol.* **1980**, *75*, 357-359.

(5) Zhao, R.; Goldman, I.D. Resistance to antifolates. *Oncogene* **2003**, *22*, 7431-7457.

(6) Assaraf, Y.G. Molecular basis of antifolate resistance. *Cancer Metastasis Rev.* **2007**, *26*, 153-181.

(7) Navarro-Perán, E.; Cabezas-Herrera, J.; García-Cánovas, F.; Durrant, M.C.; Thorneley, R.N.F.; Rodríguez-López, J.N. The antifolate activity of tea catechins. *Cancer Res.* **2005**, *65*, 2059-2064.

(8) Alemdaroglu, N.C.; Wolffram, S.; Boissel, J.P.; Closs, E.; Spahn-Langguth, H.; Langguth, P. Inhibition of folic acid uptake by catechins and tea extracts in Caco-2 cells. *Planta Med.* **2007**, *73*, 27-32.

(9) Spina, M.; Cuccioloni, M.; Mozzicafreddo, M.; Montecchia, F.; Pucciarelli, S.; Eleuteri, A.M.; Fioretti, E.; Angeletti, M. Mechanism of inhibition of wt-dihydrofolate reductase from E. coli by tea epigallocatechin-gallate. *Proteins* **2008**, *72*, 240-251.

(10) Kao, T.T.; Wang, K.C.; Chang, W.N.; Lin, C.Y.; Chen, B.H.; Wu, H.L.; Shi, G.Y.; Tsai, J.N.; Fu, T.F. Characterization and comparative studies of zebrafish and human recombinant dihydrofolate reductases--inhibition by folic acid and polyphenols. *Drug. Metab. Dispos.* **2008**, *36*, 508-516.

(11) Hannewald, P.; Maunit, B.; Muller, J.F. Screening of DHFR-binding drugs by MALDI-TOFMS. *Anal. Bioanal. Chem.* **2008**, *392*, 1335-1344.

(12) Hong, J.; Lu, H.; Meng, X.; Ryu, J.H.; Hara, Y.; Yang, C.S. Stability, cellular uptake, biotransformation, and efflux of tea polyphenol (-)-epigallocatechin-3-gallate in HT-29 human colon adenocarcinoma cells. *Cancer Res.* **2002**, *62*, 7241-7246.

(13) Sánchez-del-Campo, L.; Otón, F.; Tárraga, A.; Cabezas-Herrera, J.; Chazarra, S.; Rodríguez-López, J.N. Synthesis and biological activity of a 3,4,5-trimethoxybenzoyl ester analogue of epicatechin-3-gallate. *J. Med. Chem.* **2008**, *51*, 2018-2026.

(14) Sánchez-del-Campo, L.S.; Rodríguez-López, J.N. Targeting the methionine cycle for melanoma therapy with 3-O-(3,4,5-trimethoxybenzoyl)-(-)-epicatechin. *Int. J. Cancer* **2008**, *123*, 2446-2455.

(15) Smith, S.L.; Patrick, P.; Stone, D.; Phillips, A.W.; Burchall, J.J. Porcine liver dihydrofolate reductase: purification, properties, and amino acids sequence. *J. Biol. Chem.* **1979**, *254*, 11475-11484.

(16) Yurkow, E.J.; Laskin, J.D. Purification of tyrosinase to homogeneity based on its resistance to sodium dodecyl sulfate-proteinase K digestion. *Arch. Biochem. Biophys.* **1989**, *275*, 122-129.

(17) Navarro-Perán, E.; Cabezas-Herrera, J.; Hiner, A.N.P.; Sadunishvili, T.; Garcia-Canovas, F.; Rodriguez-Lopez, J.N. Kinetics of the inhibition of bovine liver dihydrofolate reductase by tea catechins: origin of slow-binding inhibition and pH studies. *Biochemistry* **2005**, *44*, 7512-7525.

(18) Berman, H.M.; Westbrook, J.; Feng, Z.; Gilliland, G.; Bhat, T.N.; Weissig, H.; Shindyalov, I.N.; Bourne, P.E. The protein data bank. *Nucleic Acids Res.* **2000**, *28*, 235-242.

(19) Cody, V.; Luft, J.R.; Pangborn, W.; Gangjee, A.; Queener, S.F. Structure determination of tetrahydroquinazoline antifolates in complex with human and *Pneumocystis carinii* dihydrofolate reductase: correlations between enzyme selectivity and stereochemistry. *Acta Crystallogr. D Biol. Crystallogr.* **2004**, *60*, 646-655.

(20) Leamon, C.P.; Low, P.S. Delivery of macromolecules into living cells: a method that exploits folate receptor endocytosis. *Proc. Natl. Acad. Sci. USA* **1991**, *88*, 5572-5576.

(21) Doucette, M.M.; Stevens, V.L. Folate receptor function is regulated in response to different cellular growth rates in cultured mammalian cells. *J. Nutr.* **2001**, *131*, 2819-2825.

(22) Ancans, J.; Tobin, D.J.; Hoogduijn, M.J.; Smit, N.P.; Wakamatsu, K.; Thody, A.J. Melanosomal pH controls rate of melanogenesis, eumelanin/phaeomelanin ratio and melanosome maturation in melanocytes and melanoma cells. *Exp. Cell Res.* **2001**, *268*, 26-35.

(23) Kong, K.H.; Park, S.Y.; Hong, M.P.; Cho, S.H. Expression and characterization of human tyrosinase from a bacterial expression system. *Comp. Biochem. Physiol.* **2000**, *125*, 563-569.

(24) Fenoll, L.G.; Rodríguez-López, J.N.; García-Sevilla, F.; Tudela, J.; García-Ruiz, P.A.; Varón, R.; García-Cánovas, F. Oxidation by mushroom tyrosinase of monophenols generating slightly unstable *o*-quinones. *Eur. J. Biochem.* **2000**, *267*, 5865-5878.

(25) Gulsen, A.; Turan, B.; Makris, D.; Kefalas, P. Copper(II)-mediated biomimetic oxidation of quercetin: generation of a naturally occurring oxidation product and evaluation of its in vitro antioxidant properties. *Eur. Food Res. Technol.* **2007**, *225*, 435-441.

(26) Navarro-Martínez, M.D.; Cabezas-Herrera, J.; García-Cánovas, F.; Rodríguez-López, J.N. Inhibition of *Stenotrophomonas maltophilia* dihydrofolate reductase by methotrexate: A single slow-binding process. *J. Enz. Inhibit. Med. Chem.* **2007**, *22*, 377-382.

(27) Appleman, J.R.; Prendergast, N.; Delcamp, T.J.; Freisheim, J.H.; Blakley, R.L. Kinetics of the formation and isomerization of methotrexate complexes of recombinant human dihydrofolate reductase. *J. Biol. Chem.* **1988**, *263*, 10304-10313.

(28) Gaukroger, J.; Wilson, L.; Stewart, M.; Farid, Y.; Habeshaw, T.; Harding, N.; Mackie, R. Paradoxical response of malignant melanoma to methotrexate in vivo and in vitro. *Br. J. Cancer.* **1983**, *47*, 671-679.

(29) Jung, Y.D.; Ellis, L.M. Inhibition of tumour invasion and angiogenesis by epigallocatechin-gallate (EGCG), a major component of green tea. *Int. J. Exp. Path.* **2001**, *82*, 309-316.

(30) Rodríguez López, J.N.; Tudela, J.; Varón, R.; García Carmona, F.; García Cánovas, F. Analysis of a kinetic model for melanin biosynthesis pathway. *J. Biol. Chem.* **1992**, *267*, 3801-3810.

(31) Ma, D.; Huang, H.; Moscow, J.A. Down-regulation of reduced folate carrier gene (RFC1) expression after exposure to methotrexate in ZR-75-1 breast cancer cells. *Biochem. Biophys. Res. Commun.* **2000**, *279*, 891-897.

(32) Tse, A.; Moran, R.G. Cellular folates prevent polyglutamation of 5, 10-dideaza-tetrahydrofolate. A novel mechanism of resistance to folate antimetabolites. *J. Biol. Chem.* **1998**, *273*, 25944-25952.

(33) Navarro-Peran, E.; Cabezas-Herrera, J.; Sánchez-del-Campo, L.S.; Rodríguez-López, J.N. Effects of folate cycle disruption by the green tea polyphenol epigallocatechin-3-gallate. *Int. J. Biochem. Cell Biol.* **2007**, *39*, 2215-2225.

(34) Rooseboom, M.; Commandeur, J.N.M.; Vermeulen, N.P.E. Enzyme-catalyzed activation of anticancer prodrugs. *Pharmacol. Rev.* **2004**, *56*, 53-102.

(35) Graffner-Nordberg, M.; Kolmodin, K.; Aqvist, J.; Queener, S.F.; Hallberg, A. Design, synthesis, and computational affinity prediction of ester soft drugs as inhibitors of dihydrofolate reductase from Pneumocystis carinii. *Eur. J. Pharm. Sci.* **2004**, *22*, 43-54.

Table 1. Inhibition constants for rHDHFR

Inhibitor	K_I (nM)	k_{on} ($M^{-1}s^{-1}$)	k_{off} (s^{-1})	Decrease by further EI reactions (-fold)	K_I^* (nM)
EGCG	920	1.3×10^5	0.12	28	33
ECG	1780	1.7×10^5	0.30	19	92
TMECG	2100	1.4×10^5	0.29	19	110
MTX[a]	0.21	4.0×10^8	0.021	60	0.0035
QM	8.2	5.8×10^4	4.8×10^{-4}	0	8.2

[a]Data obtained from[27]

Legend to Charts

Chart 1. Reaction sequences indicating the oxidation of TMECG by TYR and the formation of quinone methide species.

Legend to Figures

Figure 1. Effect of TMECG on several epithelial cell lines and expression of TYR in normal and pathological melanocytes: (a) TMECG-half maximal inhibitory concentration (IC_{50}) on several melanoma and non-melanoma cells after 7 days of treatment. The figure also shows the dependence of TMECG-IC_{50} on cell doubling time; (b) Semiquantitative determination of TYR mRNA. Histograms represent the logarithm of the number of copies of TYR mRNA for each 1×10^3 copies of β-actin. The insert are western blot for TYR and β-actin analysis in normal and pathological melanocytes and the picture is from a representative experiment repeated 3 times with similar results.

Figure 2. Effects of TYR silencing on TMECG action and enhanced activity of TMECG on Caco-2 cells after targeted delivery of TYR: (a) TYR silencing and siRNA prevention of the antiproliferative action of TMECG (20 and 50 μM) on SkMel-28 cells. Western blot was performed 72 h after siRNA transfection and the percentage of TYR expression was calculated with respect to TYR expression in siRNA-untreated control cells (CN); (b) Folate-conjugated TYR is taken up by Caco-2 cells via folate receptor-mediated endocytosis as demonstrated by confocal microscopy and by flow-cytometry using TYR-FITC and FOL-TYR-FITC; (c) Folate-conjugated TYR efficiently activates TMECG in Caco-2 cells. As demonstrated by the appropriate controls, only the combination of FOL-TYR/TMECG reduced viability and induced apoptosis in Caco-2 cells. Significance of the results was determined via the paired *t*-test between the TMECG-treated cells in the absence of TYR and in the presence of the folate-conjugated enzyme.

Figure 3. TYR-catalyzed oxidation of TMECG in 30 mM sodium acetate buffer, pH 5.5, 25ºC: (a) Spectrophotometric recordings for the oxidation of TMECG (0.2 mM) in the presence of human TYR (0.5 μg/mL). The arrow represents the absorbance direction and the time between recordings was 1 min; (b) Effect of TMECG concentration on the initial rate of

human TYR (0.5 μg/mL). Data were fitted to the Michaelis-Menten equation using non-linear regression analysis; (c) Effect of pH on QM (50 μM) absorbance at 480 nm.

Figure 4. rHDHFR binding and inhibition studies: (a) Titration fluorescence experiments for the binding of QM to rHDHFR (0.5 μM). The inset shows a comparison of the rHDHFR fluorescence quenching by MTX and TMECG under the same assay conditions; (b) Progress curves for the irreversible inhibition of rHDHFR by QM; (c) Dependence of the pseudo-first-order rate constant (k_{obs}) for the binding of TMECG and QM to rHDHFR on inhibitor concentration; (d) Progress curves for the recovery of the rHDHFR activity after preincubation with TMECG or QM; (e) Molecular modeling for the binding of TMECG and QM (as $QM^{\ominus}$) to human DHFR.

Figure 5. Reversion experiments and effects of TMECG on RFC and DHFR expression: (a) Effects of 0.1 mM leucovorin (LV) and HT-medium on the antiproliferative activity of 20 μM TMECG on SkMel-28 melanoma cells after 3 days of drug exposition. The data are expressed assuming 100% cell viability for the untreated controls. Statistical comparisons between TMECG-treated cells in the different situations are included (*ns*, not significant); (b) Time-dependent expression of RFC mRNA in SkMel-28 after 20 μM TMECG treatments. Histogram bars (± SD) represent the number of copies of DHFR mRNA for every 1 x 10^3 copies of β-actin. The figure also shows the differences in RFC mRNA expression between HeM and SkMel-28 (zero time) and the RFC protein levels in HeM, SkMel-28 cells (Sk28), and SkMel-28 cells treated for 3 days with 20 μM TMECG; (c) Differential effects of TMECG and MTX on DHFR mRNA and protein expression in SkMel-28 melanoma cells. The upper panel represents RT-PCR analysis of mRNA DHFR in normal melanocytes (HeM), untreated SkMel-28 cells, and SkMel-28 cells treated for 3 days with 20 μM TMECG or 1 μM MTX. Histogram bars (± SD) represent the number of copies of DHFR mRNA for every 1 x 10^6 copies of β-actin. Data were obtained from five mRNA determinations in three individual experiments. DHFR protein levels (lower panel) determined by western blot analysis and using β-actin as an internal control. Pictures are from a representative experiment repeated three times with similar results.

Figure 6. Inhibition of melanoma growth and metastasis by TMECG: (a) Median survival time following tumor implantation; (b) Mean tumor size in C57/B16 mice bearing B16 melanomas. Analysis was stopped when the number of survivors dropped below five per group. The difference between untreated and TMECG-treated groups at day 21 was significant ($p < 0.05$). The images show tumor size after day 18 from tumor cell injection in control and TMECG-treated mice; (c) Rate of metastasis in postmortem and histological examination of lungs showing general aspect and histopathological analysis of lungs from C57/B16 mice bearing the B16 melanoma in control and TMECG-treated animals.

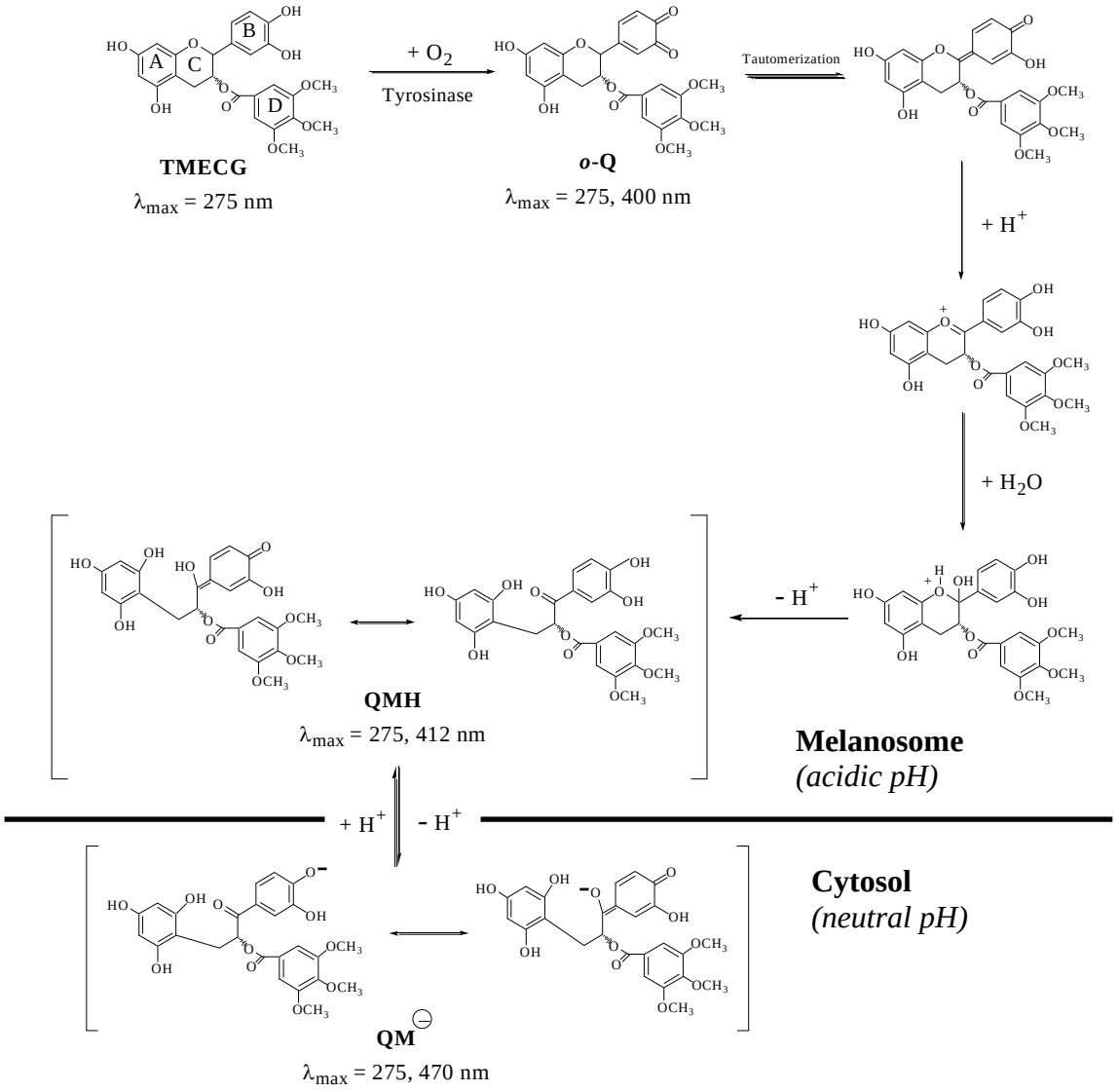

Chart 1. **Sánchez-del-Campo et al.**

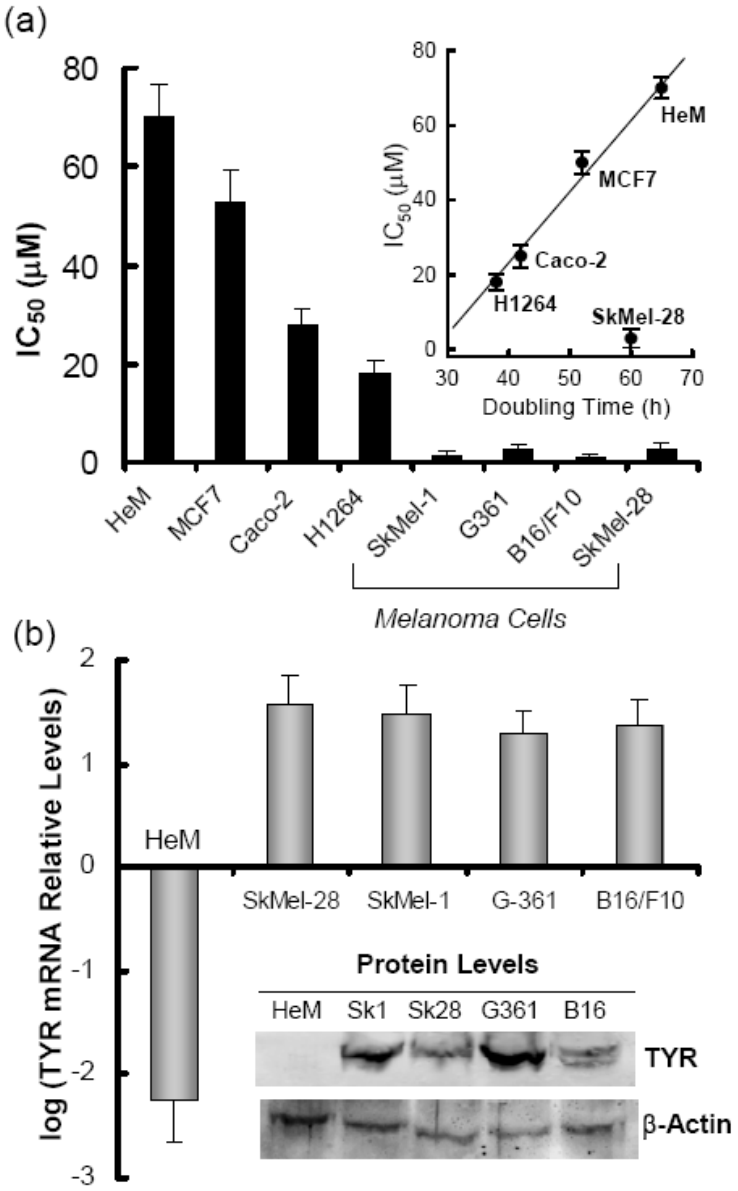

Figure 1. **Sánchez-del-Campo et al.**

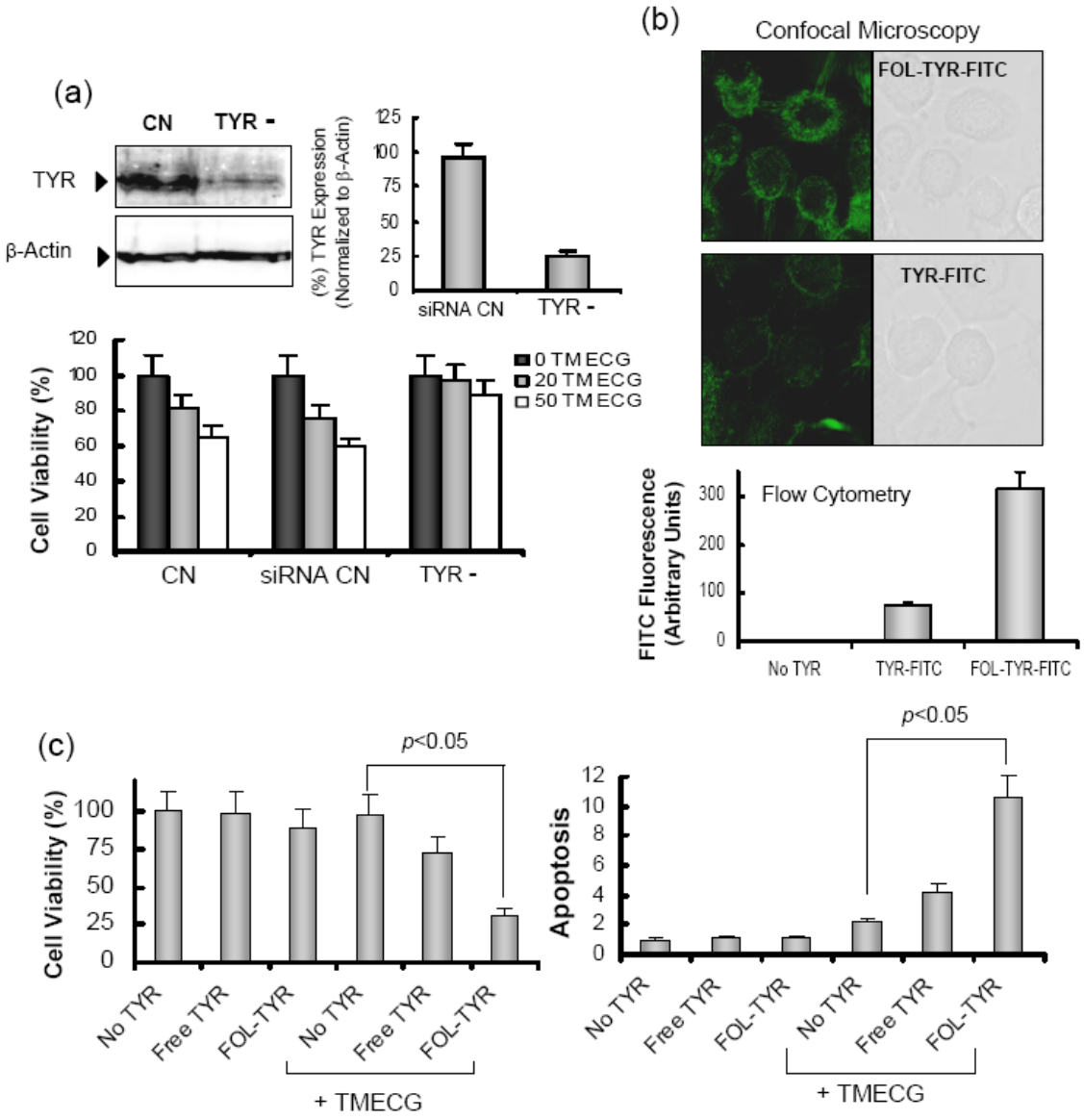

Figure 2. **Sánchez-del-Campo et al.**

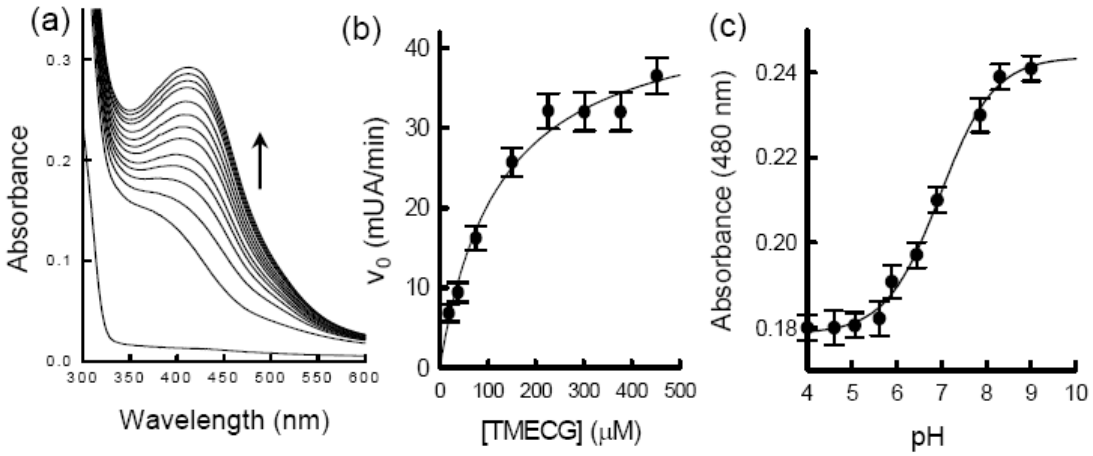

Figure 3. **Sánchez-del-Campo et al.**

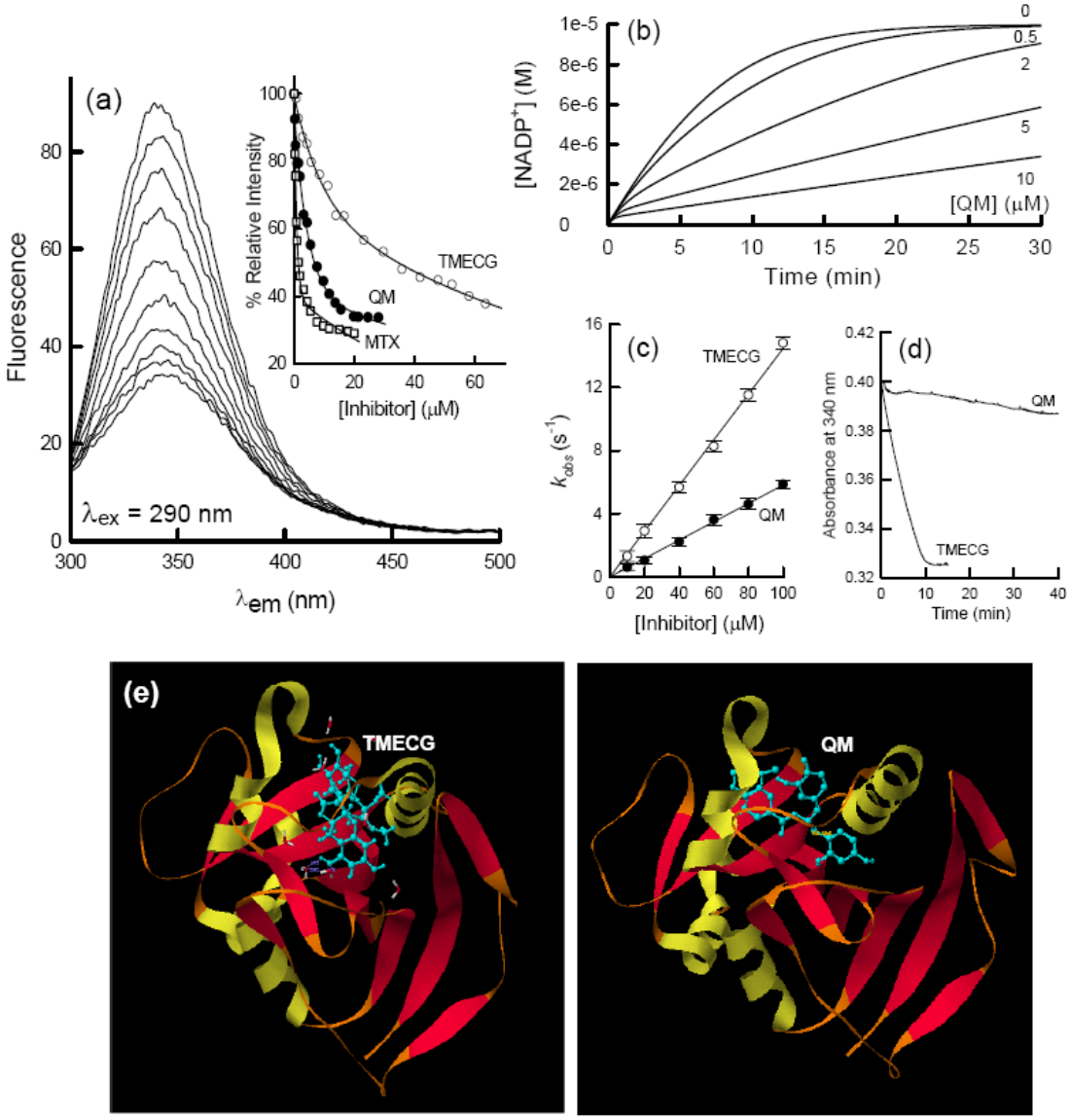

Figure 4. **Sánchez-del-Campo et al.**

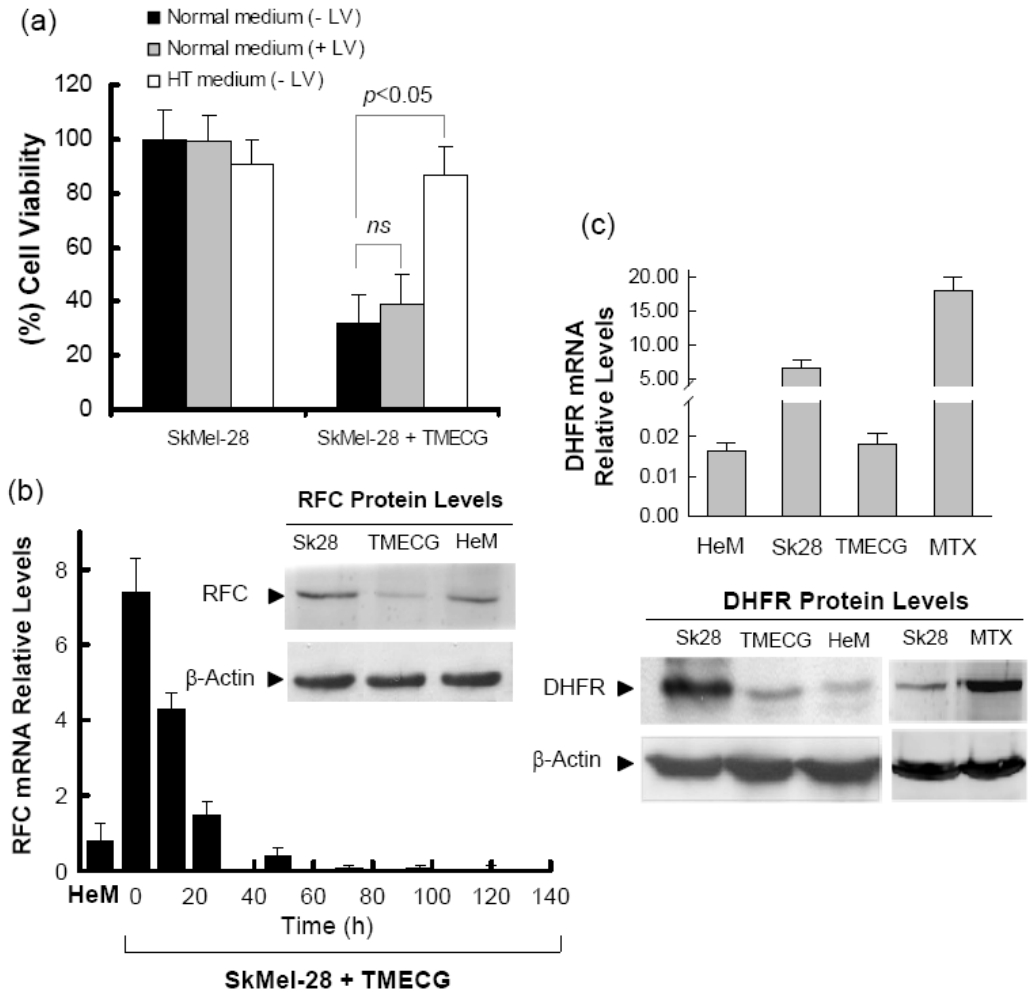

Figure 5. **Sánchez-del-Campo et al.**

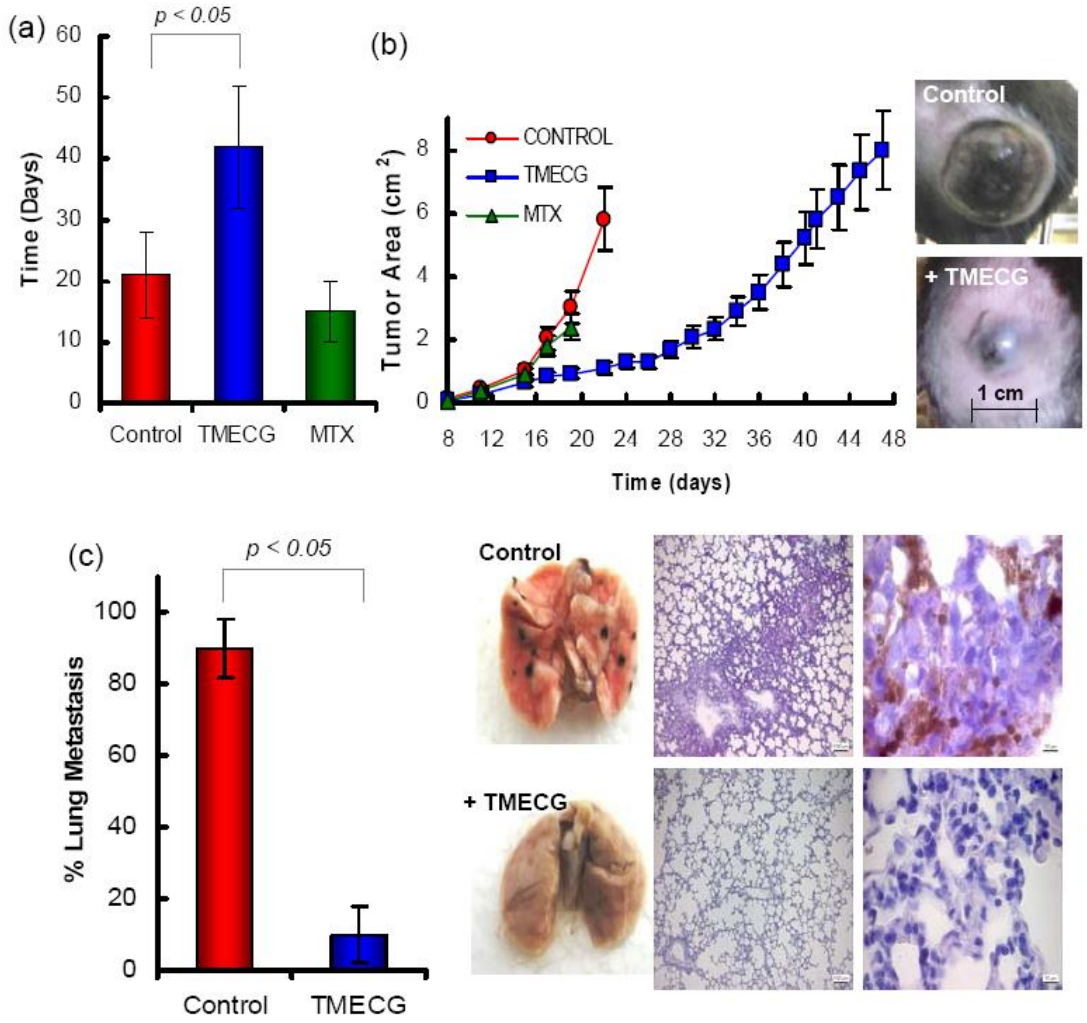

Figure 6. **Sánchez-del-Campo et al.**

For Table of Contents Use Only

Melanoma Activation of 3-*O*-(3,4,5-Trimethoxybenzoyl)-(-)-Epicatechin to a Potent Irreversible Inhibitor of Dihydrofolate Reductase

Luís Sánchez-del-Campo, Alberto Tárraga, María F. Montenegro, Juan Cabezas-Herrera, and José Neptuno Rodríguez-López